# Performance Comparison of Uplink WLANs with Single-user and Multi-user MIMO Schemes

Hu Jin, Bang Chul Jung, Ho Young Hwang, and Dan Keun Sung
CNR Lab., School of EECS., KAIST
373-1, Guseong-dong, Yuseong-gu, Daejeon, 305-701, KOREA
Email: {jinhu, bcjung, hyhwang}@cnr.kaist.ac.kr; dksung@ee.kaist.ac.kr

*Abstract*— **In this paper, we compare the performance of wireless local area networks (WLANs) with single-user MIMO (SU-MIMO) and multi-user MIMO (MU-MIMO) in terms of collision probability, average throughput, and delay. In the SU-MIMO scheme, multiple antennas are used for transmitting multiple data streams of a *single user* and this MIMO technique increases link capacity at physical (PHY) layer. In the MU-MIMO scheme, however, multiple antennas at different users are used for transmitting data streams of *multiple users*. The MU-MIMO scheme reduces the collision probability at medium access control (MAC) layer and increases the link capacity. Both MIMO schemes yield different collision, throughput, and delay performance at the MAC layer of WLANs. Numerical results show that the MU-MIMO scheme yields lower collision probability and shorter delay performance than the SU-MIMO scheme. Furthermore, the SU-MIMO scheme yields better throughput performance for high SNR values and a small number of contending stations. In other cases, the MU-MIMO scheme yields better throughput performance.**

## I. Introduction

For wireless local area network (WLAN) systems [1], most studies on medium access control (MAC) layer have been done under the assumption of a simple collision model in which frame errors occur when there are simultaneous transmissions from multiple stations [2]–[5]. However, this collision model did not exactly describe the physical (PHY) layer characteristics of WLAN systems because a frame is assumed to arrive at the receiver without an error when only a single station transmit its frame. In practice, in this collision model, channel effects such as fading and noise at the receiver are not considered and frames may be successfully decoded even in the presence of simultaneous transmissions.

Tong *et al.* [6] modified this simple collision model considering advances in multiuser communications at the PHY layer and investigated the MAC layer performance when a multi-packet reception (MPR) scheme is applied in ALOHA systems. However, they only provided a theoretical possibility that a packet is successfully decoded when the MPR is used at the receiver. Recently, Jin *et al.* [7] proposed a collision mitigation scheme in uplink WLANs using multiple antennas at the access point (AP). We here utilize multiple input multiple output (MIMO) detection techniques at the AP when multiple users simultaneously transmit their frames. As a result, the collision model in WLAN systems needs to be modified with MIMO techniques.

On the other hand, MIMO transmission techniques have been adopted by many systems to achieve high spectral efficiency in recent years [8]–[11]. Transmission data rates can be increased by simultaneously transmitting several independent data streams through different antennas, which is called *spatial multiplexing*. If these multiple data streams are originated from a single transmitter, as shown in Fig.1(a), then we call it single-user MIMO (SU-MIMO) multiplexing in this paper. If the transmitted data streams are originated from different transmitters, as shown in Fig.1(b), we call it multi-user MIMO (MU-MIMO) multiplexing for comparison. The SU-MIMO scheme is adopted by the IEEE 802.11n specification [11], while the MU-MIMO is not adopted. Mirkovic and Orfanos [12] proposed a new MAC protocol for SU-MIMO based WLANs and showed the performance results. They focused on the performance improvement of PHY layer through the MIMO techniques. However, they did not consider the MIMO techniques as a collision mitigation scheme at the MAC layer. For the MU-MIMO schemes, Wang and Tureli [13] showed one example of the MU-MIMO schemes and introduced a new MAC, called multiple antennas receiver initiated busy tone medium access (MARI-BTMA) in an ad hoc network and evaluated the performance.

Although there have been many studies adopting MIMO techniques for WLAN systems, the performance of WLAN systems with an SU-MIMO scheme and an MU-MIMO scheme has not been compared yet. In this paper, we compare the performance of two MIMO schemes in WLAN systems. To compare the performance, we first evaluate the theoretical capacity for both MIMO schemes at the PHY layer in a Rayleigh fading environment. Since the current IEEE 802.11 MAC does not support the MU-MIMO scheme, we proposed a small change in the current MAC protocol for adopting the MU-MIMO scheme. In order to analyze the MAC layer performance, we have extended Bianchi's [2] discrete time Markov chain (DTMC) model to support the MU-MIMO schemes. Therefore, we compare the cross layer performance of these two schemes in this paper.

The rest of this paper is organized as follows: In Section II, the theoretical capacities of both the SU-MIMO and MU-MIMO schemes are derived when the receiver uses a zero-forcing (ZF) detection scheme. In Section III, the MU-MIMO scheme supporting MAC is proposed and the extended DTMC model is proposed. In Section IV, numerical results are pre-

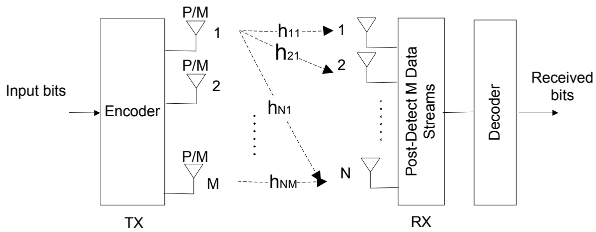


(a) Single-user MIMO

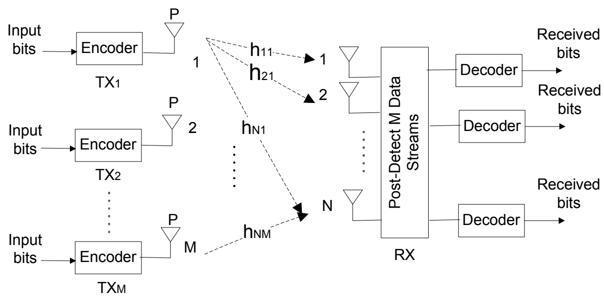


(b) Multi-user MIMO

Fig. 1. System model

sented to compare the performance of the SU-MIMO and MU-MIMO schemes. Finally, conclusions are presented in Section V.

## II. Ergodic capacity of Both SU-MIMO and MU-MIMO schemes

Fig. 1 shows two MIMO system models in which one is based on an SU-MIMO scheme and another is based on an MU-MIMO scheme. In the SU-MIMO scheme, input bits are first encoded with one encoding block and are transmitted through $M$ parallel antennas. The received signals through $N$ antennas are first post-detected into $M$ data streams and are decoded by one decoding block at the receiver side, as shown in Fig.1(a). On the other hand, in the MU-MIMO scheme, input bits are encoded independently at each user's encoder and are transmitted through each user's transmitter antenna. At the receiver side, $M$ independent data streams are post-detected and decoded independently, as shown in Fig.1(b). In the power limited wireless system, the power assigned to each antenna is averaged by the number of transmitter antennas $M$ in the SU-MIMO scheme, while the transmitter power is allocated differently to each transmitter antenna in the MU-MIMO scheme. Although each user can have several antennas with MU-MIMO scheme, we assume each user has one antenna to transmit data streams in this paper.

For both schemes, the channel matrix $\boldsymbol{H}$ can be expressed as

$$\boldsymbol{H} = [\boldsymbol{h}_1, \boldsymbol{h}_2, \cdots, \boldsymbol{h}_M], \tag{1}$$

where $\boldsymbol{h}_i = (h_{1i}h_{2i}\cdots h_{Ni})^T$ denotes the channel gain from the $i$-th transmitter antenna to the $N$ antennas of the receiver. With Rayleigh fading, $h_{ji}(j = 1, 2, \cdots, N)$ is an independent, zero-mean, complex Gaussian random variable with a variance of $2\sigma_i^2$. In the SU-MIMO scheme, each variance, $2\sigma_i^2 (i = 1, 2, \cdots, M)$, is identical, while they may have different values for the MU-MIMO scheme, because the different transmitters can have varying distances away from the receiver. The received signal at the receiver can be written as

$$\boldsymbol{r} = \boldsymbol{H}\boldsymbol{s} + \boldsymbol{n}, \tag{2}$$

where $\boldsymbol{s} = (s_1 s_2 \cdots s_M)^T$ and $\boldsymbol{r} = (r_1 r_2 \cdots r_N)^T$ represent the transmitted and received symbol vectors, respectively. The term $\boldsymbol{n}$ is a complex Gaussian vector in which each component has zero mean and variance $N_0$. Using the channel gain $\boldsymbol{H}$, the receiver can recover the transmitted symbols by using MIMO decoding techniques. Joint maximum likelihood (ML) decoding yields the best performance, but its complexity increases exponentially as the number of transmitted data streams increases. A zero forcing (ZF) detection uses a simple matrix inversion. The ZF matrix filter separates the received symbol vectors into their transmitted streams and it is given by

$$\boldsymbol{G}_{ZF} = \boldsymbol{H}^\dagger = (\boldsymbol{H}^H\boldsymbol{H})^{-1}\boldsymbol{H}^H, \tag{3}$$

where $\boldsymbol{H}^\dagger$ is the pseudo-inverse matrix and $\boldsymbol{H}^H$ is a Hermitian matrix which is the conjugate transpose of matrix $\boldsymbol{H}$. Since we assume the elements of $\boldsymbol{H}$, $h_{ji}$, are independent of each other and $N \geq M$, the channel matrix $\boldsymbol{H}$ is of full column rank and, consequently, $\boldsymbol{G}_{ZF}$ is invertible.

For a given transmitted symbol vector $\boldsymbol{s} = (s_1 s_2 \cdots s_M)^T$ and a given received symbol vector $\boldsymbol{r} = (r_1 r_2 \cdots r_N)^T$, the output of the ZF receiver is given by

$$\hat{\boldsymbol{s}} = \boldsymbol{G}_{ZF}\boldsymbol{r} = \boldsymbol{H}^\dagger(\boldsymbol{H}\boldsymbol{s} + \boldsymbol{n}) = \boldsymbol{s} + \boldsymbol{z}, \tag{4}$$

where $\boldsymbol{z} = \boldsymbol{H}^\dagger\boldsymbol{n}$. Then, the covariance matrix of $\boldsymbol{z}$, $\boldsymbol{K}$ is obtained as

$$\boldsymbol{K} = E[\boldsymbol{z}\boldsymbol{z}^*] = \boldsymbol{H}^\dagger(\boldsymbol{H}^\dagger)^H N_0 = (\boldsymbol{H}^H\boldsymbol{H})^{-1}N_0. \tag{5}$$

From the definition of covariance matrix $\boldsymbol{K}$, we can obtain

$$E[z_i z_i^*] = E[|z_i|^2] = K_{ii} = [(\boldsymbol{H}^H\boldsymbol{H})^{-1}]_{ii}N_0, \tag{6}$$

where $[A]_{ii}$ is the element in the $i$-th row and the $i$-th column. Thus, the post-detection signal-to-noise Ratio (SNR) for the $i$-th data symbol, $\gamma_i$, is given by the following equation:

$$\gamma_i = \frac{E[|s_i|^2]}{E[|z_i|^2]} = \frac{E[|s_i|^2]}{[(\boldsymbol{H}^H\boldsymbol{H})^{-1}]_{ii}N_0} = \frac{\gamma_0}{[(\boldsymbol{H}^H\boldsymbol{H})^{-1}]_{ii}}, \tag{7}$$

where $\gamma_0$ is defined as $E[|s_i|^2]/N_0$. Although the variance of each column of $\boldsymbol{H}$ can be different, the statistical property of $1/[(\boldsymbol{H}^H\boldsymbol{H})^{-1}]_{ii}$ is not affected by other columns and it has a Chi-square distribution with $2(N-M+1)$ degrees of freedom and variance $\sigma_i^2$ [14]. Consequently, the post-detection SNR

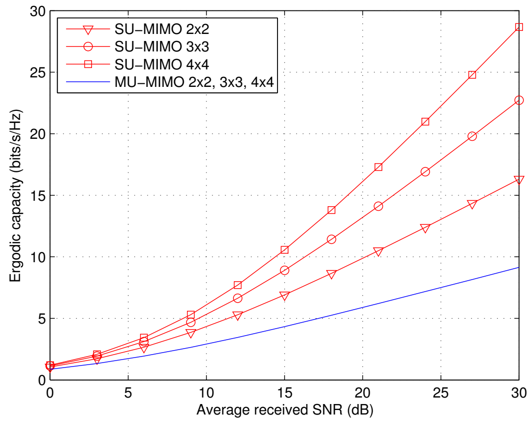


Fig. 2. Ergodic capacity of a single user

for the $i$-th transmitter, $\gamma_i (1 \leq i \leq M)$ has a probability density function (PDF) of

$$f_{2(N-M+1)}(\gamma_i) = \frac{\exp(-\frac{\gamma_i}{2\sigma_i^2\gamma_0})}{(N-M)!(2\sigma_i^2\gamma_0)^{N-M+1}} \times \left(\frac{\gamma_i}{2\sigma_i^2\gamma_0}\right)^{N-M}. \quad (8)$$

Eq. (8) shows that the post-detection SNR for the $i$-th data stream only depends on its own channel variance $\sigma_i^2$ and it is not affected by other data streams. However, an increase in the number of transmitting data streams, $M$, reduces the degrees of freedom.

The ergodic capacity can be obtained from the post-detection SNR distribution. The channel capacity through the $i$-th transmitter antenna, $C_i$[bit/s/Hz] is

$$C_i = \int_0^\infty \log_2(1+\gamma_i) f_{2(N-M+1)}(\gamma_i) d\gamma_i. \quad (9)$$

Eq. (9) can be further simplified [15]. An integral form $I_m(\mu)$ has the following characteristic:

$$\begin{aligned} I_m(\mu) &= \int_0^\infty t^{m-1} \ln(1+t) \exp(-\mu t) dt \\ &= (m-1)! \cdot \exp(\mu) \sum_{k=1}^{m} \frac{\Gamma(-m+k,\mu)}{\mu^k}, \end{aligned} \quad (10)$$

where $\Gamma(\cdot,\cdot)$ is the complementary incomplete gamma function defined as

$$\Gamma(\alpha, x) = \int_x^\infty t^{\alpha-1} \exp(-t) dt.$$

Then, we can rewrite $C_i$ as

$$C_i = \frac{1}{(N-M)! \cdot \bar{\gamma}_i^{N-M+1}} \log_2(e) I_{N-M+1}\left(\frac{1}{\bar{\gamma}_i}\right), \quad (11)$$

where the average received SNR $\bar{\gamma}_i$ is defined as $2\sigma_i^2\gamma_0$. The capacity specified by Eq.(11) is the maximum achievable spectral efficiency in an error-free and we assume this capacity can be obtained by gaussian coding in later analysis.

Fig. 2 shows each user's ergodic capacity for both MIMO schemes with varying numbers of transmitter and receiver antennas. In the case of the MU-MIMO scheme, if the number of transmitters, $M$, is equal to the number of receiver antennas, $N$, the capacities are identical for all users. But for the SU-MIMO scheme, the capacity is increased with an increase in the number of transmitter and receiver antennas. From the viewpoint of each user, the SU-MIMO scheme yields much better ergodic capacity than the MU-MIMO scheme. With this PHY layer performance, we will compare the MAC layer performance in Section III.

## III. Performance Analysis of CSMA/CA with a Binary Exponential Backoff Protocol

### A. Description of MAC Protocol

IEEE 802.11 series wireless LANs adopt a CSMA/CA protocol with binary exponential backoff. Fig. 3(a) shows a simple example of the procedure of CSMA/CA protocol with a binary exponential backoff algorithm. All stations(STAs) take a backoff procedure after their shared channel is idle during a DCF interframe space (DIFS) period. Each STA randomly chooses an integer value as a backoff counter value in a contention window of $(0, CW-1)$, where $CW$ is the contention window size and is initially set to a minimum value $CW_{\min}$. In the backoff procedure, the backoff counter value is decreased by one for each idle $SlotTime$ and it is frozen if the channel is occupied by other STAs. An STA with a backoff counter value of 0 can transmit a frame. After the successful transmission, the STA can receive an acknowledgement (ACK) frame from the receiver after a short interframe space (SIFS) period. If the transmitted frame collides with other frames as shown in Fig. 3(b), then the STA can not receive an ACK frame from the receiver. In order to retransmit the failed frame, the STA doubles the $CW$ value and returns to a backoff procedure after an ACK timeout period. The $CW$ value can be increased up to a maximum value $CW_{\max}$ and there also exist a maximum retry limit for retransmission.

In order to support simultaneous transmission of the STAs, the legacy CSMA/CA protocol has to be slightly changed. As shown in Fig. 3(c), if the receiver supports MU-MIMO, the two transmitted data can be correctly recovered by the receiver and it has to send two ACK frames to each STA within the SIFS time. Since the data transmission time for each STA can be different, the ACK frames have to be sent after the complete transmission of both data frames. If the receiver can recover $N$ simultaneous data streams, it has to send $N$ ACK frames to each STA. In this paper, each STA is assumed to have a unique preamble chosen from an orthogonal preamble sequence set. Hence, the AP knows which STA transmits its data and estimates the channel coefficients of each STA.

### B. Performance Analysis

Bianchi [2] proposed a simple DTMC model to compute the saturation throughput in a saturation traffic case. We have extended this model to accommodate simultaneous transmissions from multiple STAs at the PHY layer in a network environment where AP is located at the center in a basic service set (BSS) and $n$-contending STAs communicate with the AP. For

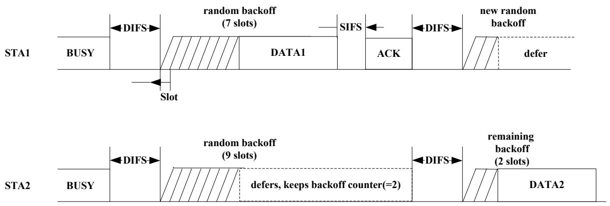


(a) Normal transmission of STA

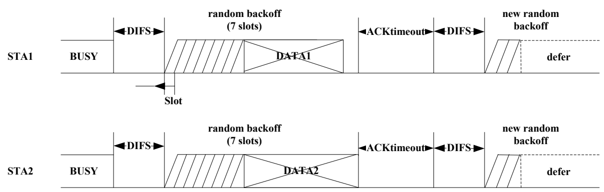


(b) Collision of two STAs

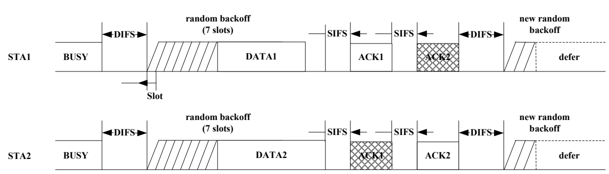


(c) Simultaneous transmission of two STAs

Fig. 3. CSMA/CA with binary exponential backoff protocol

simplicity, we assume there is only uplink transmission and no downlink transmission except the transmission of ACK frames.

For each STA, let $\tau$ be the transmission probability and $p$ be the backoff stage transition probability that the STA retransmits the previous transmitted frame. Since we assume gaussian coding is used at the PHY layer, there is no channel error and, consequently, the backoff stage transition probability is the same as the collision probability. If an AP can receive maximum $N$ simultaneous transmissions, a transmission failure occurs when there are more than $N$ simultaneous transmissions. From the viewpoint of a given backoff procedure with retry limit $R$, we can obtain the relationship between $\tau$ and $p$, based on DTMC model in [2],

$$\tau = \frac{2(1-p^{R+1})}{W(1-2^L p^{R+1}) + Wp[\sum_{i=0}^{L-1}(2p)^i] + (1-p^{R+1})}, \tag{12}$$

where $W$ represents the minimum contention window size $CW_{\min}$. The term $L$ is the maximum number of doublings of the $CW$, which is identical to $\log_2(CW_{\max}/CW_{\min})$.

If the AP can receive maximum $N$ simultaneous transmissions from $N$ STAs together, for each STA, the backoff stage transition can occur when there are more than $(N-1)$ STAs transmitting data at the same time among remaining $(n-1)$ STAs. Consequently, the relationship between $\tau$ and $p$ from this viewpoint is,

$$p = 1 - \sum_{m=0}^{N-1} \binom{n-1}{m} \tau^m (1-\tau)^{n-1-m}, \tag{13}$$

where the probability that $m$ STAs transmit frames simultaneously among the remaining $(n-1)$ STAs is expressed as $\binom{n-1}{m}\tau^m(1-\tau)^{n-1-m}$. As a special case, $N=1$ represents the SU-MIMO scheme-based networks.

Numerically solving Eqs.(12) and (13), the transmission probability $\tau$ and backoff stage transition probability $p$ can be obtained. The probability $P_{tr}^{sys}$ that there is at least one STA's transmission in a time slot is written as

$$P_{tr}^{sys} = 1 - (1-\tau)^n. \tag{14}$$

The probability $P_{tr}^m$ that there are $m$ STAs' simultaneous transmissions in a time slot is written as

$$P_{tr}^m = \binom{n}{m} \tau^m (1-\tau)^{n-m}. \tag{15}$$

The collision probability $P_c^{sys}$ that there are more than $N$ STAs' simultaneous transmissions in a time slot is written as

$$P_c^{sys} = \sum_{m=N+1}^{n} P_{tr}^m. \tag{16}$$

The average payload size for a successful transmission in data transmission time is obtained as

$$E[\text{payload}] = \sum_{m=1}^{N} m \cdot P_{tr}^m \cdot E[P_{scheme}], \tag{17}$$

where $E[P_{scheme}]$ is the average payload size which is transmitted by one STA during data transmission time under specified PHY layer transmission schemes, such as SU-MIMO and MU-MIMO. Then, the average throughput can be obtained as

$$\begin{aligned} \text{Throughput} &= \frac{E[\text{payload transmitted in a time slot}]}{E[\text{length of a time slot}]} \\ &= \frac{E[\text{payload}]}{(1-P_{tr}^{sys})SlotTime + \sum_{m=1}^{N} P_{tr}^m T_{tr}^m + P_c^{sys} T_c}, \end{aligned} \tag{18}$$

where $SlotTime$ is the backoff slot time. $T_{tr}^m$ is the time used to transmit $m$ simultaneously transmitted frames including overhead and it is expressed as

$$\begin{aligned} T_{tr}^m &= MaxDataTime + m \cdot (SIFS + ACKtime) + DIFS \\ &= MaxDataTime + ACKtimeout + DIFS, \end{aligned}$$

where $MaxDataTime$ is the maximum data transmission time of the simultaneously transmitting STAs. $T_c$ is the time used by more than $N$ STAs' simultaneous transmissions which is considered as collision and it is expressed as

$$T_c = MaxDataTime + ACKtimeout + DIFS.$$

Delay is defined as the time interval from the instant that the first bit of a frame is transmitted from its buffer for transmission, until the instant that the last bit of the ACK

TABLE I

MAC LAYER PARAMETERS

| | |
|---|---|
| DIFS | 34 $\mu s$ |
| SlotTime | 9 $\mu s$ |
| SIFS | 16 $\mu s$ |
| ACKtime | 44 $\mu s$ |
| ACKtimeout | 60 $\mu s$ |
| PHY overhead | 20 $\mu s$ |
| $CW_{\min}$ | 16 |
| $CW_{\max}$ | 1024 |
| Retry limit | 7 |
| Bandwidth | 20 MHz |

frame is received. The delay is the same as the average waiting time in each backoff stage and is obtained as

$$\text{Delay} = \sum_{i=0}^{R}\left[\frac{\max(2^i W, CW_{\max}+1)}{2}\frac{(p^i - p^{R+1})}{1-p^{R+1}}\right]\times \left[(1-P_{tr}^{sys})SlotTime + \sum_{m=1}^{N} P_{tr}^{m}T_{tr}^{m} + P_c^{sys}T_c\right]. \quad (19)$$

## IV. NUMERICAL RESULTS

In order to compare the MAC layer performance clearly, we consider a scenario in which an AP is located in the center and there exist only uplink traffic and their corresponding ACK frames transmitted from the AP. The MAC layer parameters used for the numerical examples are summarized in Table. I and they come from IEEE 802.11a specification [16].

Fig. 4 shows the collision probability for both the SU-MIMO and MU-MIMO schemes. The collision probability is one of the most critical factors affecting the MAC layer performance such as throughput and delay. In the SU-MIMO scheme, a collision occurs if more than two STAs simultaneously transmit their frames. In the MU-MIMO scheme, as we noted in Section III-B, the collision occurs only when the number of simultaneous transmissions is larger than the number of receiver antennas at the AP. Hence, the collision probability of the MU-MIMO scheme decreases as the number of receiver antennas at the AP increases, while the collision probability in the SU-MIMO scheme does not vary according to the number of antennas at the AP. The MU-MIMO scheme yields lower collision probability than that of the SU-MIMO scheme.

In order to evaluate the performance of the system in terms of throughput and delay, we assume that the average received SNR of each STA at the AP has an identical value. Through this setting, we can focus on the performance comparison between the SU-MIMO scheme and MU-MIMO scheme. Fig. 5 shows the average throughput for varying the number of STAs and the number of receiver antennas at the AP. Figs. 5(a) and 5(c) show the throughput performance when the average received SNR value are set to 5dB and 20dB, respectively. In both figures, the payload size is set to 10000 bytes. Comparing these two figures, we can observe that the SU-MIMO scheme yields better throughput performance for high SNR values and

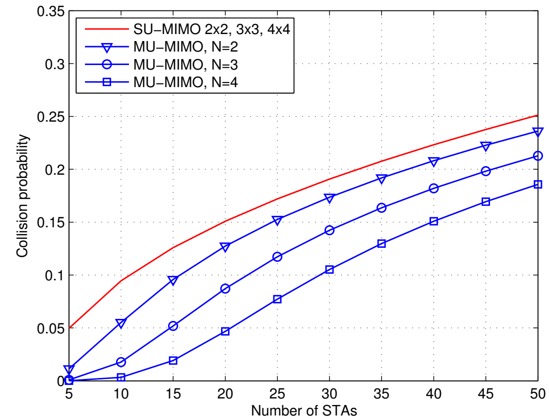


Fig. 4. Collision probability

a small number of STAs. The reasonis that the SU-MIMO scheme has much better spectral efficiency than the MU-MIMO scheme especially in the high SNR region, as shown in Fig. 2. However, as the number of STAs increases, collisions can be a dominant factor for the degradation of throughput and, consequently, the MU-MIMO scheme shows better throughput since it has lower collision probabilities. Figs. 5(b) and 5(c) show the throughput performance when the payload size are set to 1000 bytes and 10000 bytes, respectively. The received SNR value is set to 20dB. These two figures show that the payload size also affects the throughput performance. If the payload size is small enough, then the MU-MIMO scheme yields better throughput performance even in the high SNR region, which indicates that the proportion of overheads such as PHY overhead and ACK transmission becomes smaller when the MU-MIMO scheme is adopted.

Fig. 6 shows the average delay versus the number of STAs for varying the average received SNR values and the payload size. As the number of received antennas at the AP increases, the delay becomes shorter for both schemes. Moreover, the MU-MIMO scheme yields shorter delay than the SU-MIMO scheme regardless of the parameter settings.

## V. CONCLUSION

In this paper, we compared the performance of WLANs with the SU-MIMO and MU-MIMO schemes in terms of collision probability, average throughput, and average delay. The capacity is analyzed at the PHY layer in a Rayleigh fading channel and the average throughput and average delay are also analyzed at the MAC layer with the proposed extended DTMC model. From numerical results, we observe that both MIMO transmission schemes yield much better performance as the number of receiver antennas at the AP increases. The SU-MIMO scheme yields better capacity performance at the PHY layer, while the MU-MIMO scheme shows better collision probability and delay performance at the MAC layer. The SU-MIMO scheme shows better throughput performance for high SNR values and a small number of STAs. In other cases, the MU-MIMO scheme outperforms the SU-MIMO scheme.

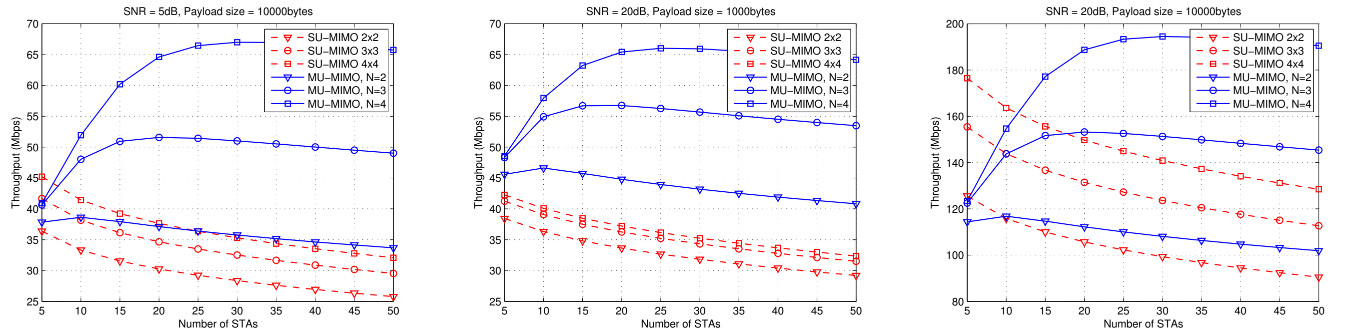


(a) Throughput when the average received SNR value is set to 5dB and the payload size is set to 10000 bytes

(b) Throughput when the average received SNR value is set to 20dB and the payload size is set to 1000 bytes

(c) Throughput when the average received SNR value is set to 20dB and the payload size is set to 10000 bytes

Fig. 5. Average throughput performance

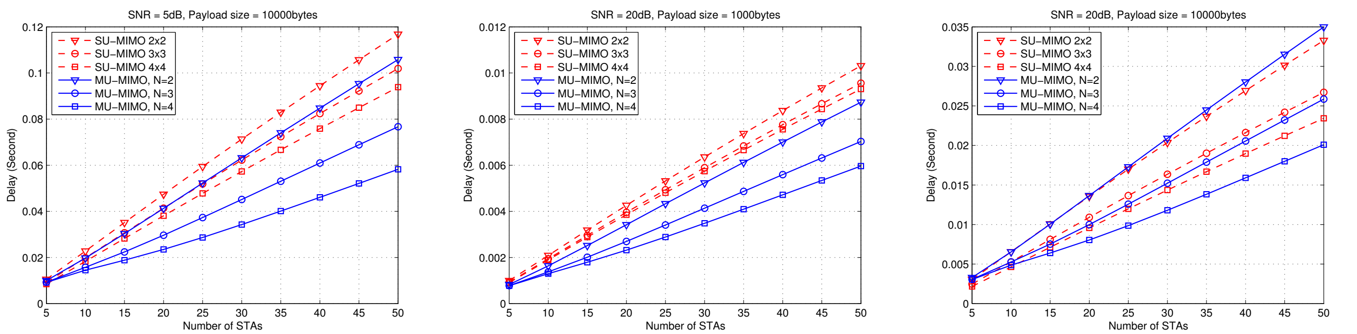


(a) Delay when the average received SNR value is set to 5dB and the payload size is set to 10000 bytes

(b) Delay when the average received SNR value is set to 20dB and the payload size is set to 1000 bytes

(c) Delay when the average received SNR value is set to 20dB and the payload size is set to 10000 bytes

Fig. 6. Average delay performance

## ACKNOWLEDGMENT

This work was supported by the center for Broadband OFDM Mobile Access (BrOMA) through the ITRC program. (IITA-2007-C1090-0701-0037)

## REFERENCES

[1] IEEE 802.11, *Part 11: Wireless LAN Medium Access Control (MAC) and Physical Layer (PHY) Specifications*, IEEE Std 802.11, Aug. 1999.

[2] G. Bianchi, “Analysis of the IEEE 802.11 distributed coordination function,” *IEEE Journal on Selected Areas in Communications,* Vol. 18, pp. 535-547, Mar. 2000.

[3] C. Wang, B. Li, and L. Li, “A new collision resolution mechanism to enhance the performance of IEEE 802.11 DCF,” *IEEE Transactions on Vehicular Technology*, Vol.53, No.4, pp. 1235- 1246, July 2004.

[4] J. Choi, J. Yoo, S. Choi, and C. Kim, “EBA: An enhancement of the IEEE 802.11 DCF via distributed reservation,” *IEEE Transactions on Mobile Computing,* Vol.4, No.4, pp. 378-390, July/August 2005.

[5] K. Kwon, Y. Fang, and H. Latchman, “A novel MAC protocol with fast collision resolution for wireless LANs,” *in Proc. IEEE INFOCOM’03*, Apr. 2003.

[6] L. Tong, V. Naware, P. Venkitasubramaniam, “ Signal processing in random access,” *IEEE Signal Processing Magazine,* Vol. 21, No. 5, pp. 29-39, Sep. 2004.

[7] H. Jin, B. C. Jung, H. Y. Hwang, D. K. Sung, “A MIMO-based Collisin Mitigatin Scheme in Uplink WLANs”, submitted to *IEEE Communications Letters.*

[8] 3GPP, TR 25.814, “Physical layer aspects for Evolved UTRA (Release 7),” Nov. 2005.

[9] IEEE C802.20-05/68r1, “MBFDD and MBTDD wideband mode: Technical overview,” Jan. 2006.

[10] IEEE, P802.16-REVd/D5, “ Part 16: Air interface for fixed broadband wireless access systems,” May 2004.

[11] IEEE P802.11n/D1.0, “Draft Amendment to Wireless LAN Media Access Control (MAC) and Physical Layer (PHY) Specifications: Enhancements for Higher Throughput,” Mar. 2006.

[12] J. Mirkovic, G. Orfanos, “A MAC Protocol for MIMO Based IEEE 802.11 Wireless Local Area Networks,” *IEEE Wireless Communications and Networking Conference, 2007,* pp. 2131-2136, 11-15 Mar. 2007.

[13] D. Wang, U. Tureli, “Cooperative MIMIO-OFDM and MAC Design for Broadband Ad Hoc Network,” *IEEE Military Communications Conference,* Vol. 1, pp. 201-207, 17-20, Oct. 2005.

[14] J. H. Winters, J. Salz, R. D. Gitlin, “The Impact of Antenna Diversity on Capacity of Wireless Communication Systems,” *IEEE Transactions on Communications* Vol. 42, no. 2/3/4, pp. 1740-1747, Feb. 1994.

[15] M-S. Alouini, A. J. Goldsmith, “Capacity of Rayleigh Fading Channels Under Different Adaptive Transmission and Diversity-combining Techniques ,” *IEEE Transactions on Vehicular Technology,* Vol. 48, No. 4, pp. 1165-1181, Jul. 1999.

[16] IEEE 802.11a,*Part 11: Wireless LAN Medium Access Control (MAC) and Physical Layer (PHY) Specifications: High-Speed Physical Layer in the 5GHz Band*, IEEE Std 802.11a, 1999.